

SG-Based Analysis of LEO Satellite-Relayed Communication Systems

Yanbo Cao, Derui Gao and Jingyu Xu

Abstract

Due to their low latency, high capacity, and seamless worldwide coverage, low Earth orbit (LEO) satellites are essential to the equal access network. Stochastic geometry (SG) is an appropriate method for such a large and irregular system. The SG model can effectively assess and estimate the performance of the network as well as handle the growing network scale. In this article, a number of common satellite distribution models are examined. In the non-technical description, system-level metrics such as coverage probability are introduced. The impact of gateway density, as well as the quantity and height of satellites, on latency and likelihood of coverage, is then researched. This essay concludes by outlining potential uses for SG in the future.

I. INTRODUCTION

Satellite system has lots of advantages such as wide coverage, large communication capacity and low transmission latency [1] [2]. In response to the disadvantage of limited terrestrial network coverage, difficulty in supporting high-speed mobile user applications, and vulnerability to natural disasters [3], satellite systems have good prospects, whether to supplement terrestrial communications or independently establish and cover the world. Therefore, within the next five years, a number of satellites will be launched into orbit, according to proposals presented by many satellite companies, such as SpaceX, Amazon, and OneWeb [4].

The following is the structure of this paper based on the description provided above. We start by going into further details about the benefits and drawbacks of LEO satellites. Then, we explain the motivation for applying SG to LEO satellite networks. In addition, a non-technical discussion of models of satellite location distribution, typical parameters, and key performance measures is provided in this paper, which reviews the analysis framework of some recent works based on SG. And most importantly, we derive some equations of T-S link in

TABLE I: Comparison of GEO-satellite, LEO-satellite and Ground System

Type of System	Capacity	Coverage area	Costs	Latency
LEO	Large	Comprehensive seamless coverage	High construction cost and high maintenance cost	Medium
GEO	Limited	Large coverage of single satellite and blind area of two poles	Low construction cost and low maintenance cost	Large
Terrestrial Network	Large	Small coverage of single base station and having difficult in the communication of specific terrain	Flexible construction and very high maintenance costs in remote areas	Low

satellite-relayed communication system. Finally, a simulation setup is suggested with valuable system-level conclusions to demonstrate the potential benefits of employing SG in modeling and assessing LEO satellite communication systems.

A. Advantages and Challenges of LEO Satellite System

Satellites are classified into high earth orbit (geostationary earth orbit, GEO), medium earth orbit (MEO) and low earth orbit satellites (LEO) according to their orbital altitude [5]. With regard to capacity, coverage, transmission delay, system design, maintenance costs, and the challenge of frequency coordination, Table I explicitly examines the benefits and drawbacks of the high orbit satellite, low orbit satellite, and ground system.

Despite a single GEO satellite that can provide a large coverage area, the conventional high orbit geostationary satellite system has blind spots at the poles. Compared to it, a constellation of LEO satellites can provide much lower latency and seamless coverage of many partially connected or unconnected areas of the globe, offering unparalleled advantages in terms of equality of access.

Although more LEO satellites are needed for seamless global connectivity, new space carriers have fortunately reduced launch costs and also assembly line production has reduced the cost of producing satellites.

The coverage of terrestrial systems is limited by the terrain. In remote areas where infrastructure is lacking, existing terrestrial networks have difficulty providing coverage because of the high cost of extending fiber to these areas. Therefore, LEO satellites offer better free-space transmission conditions and broader coverage compared to terrestrial networks. However, the design and performance analysis of the satellite constellation is particularly important because of the long deployment time and less flexibility of the satellites.

However, in the development of satellite systems, frequency resources are becoming the focus of competition among countries and satellite companies. According to current international rules,

only one satellite in orbit within a constellation gets priority for frequency and orbital resources. By developing a satellite Internet, it can easily evolve into a competition for satellite frequency resources.

The Ku and Ka frequency bands, which are used by GEO satellite constellations, are also used by LEO satellite constellations. ITU regulations state that GEO satellites have priority when it comes to frequency use, but when LEO satellites travel through the area between a GEO satellite and its customers or gateways, there is an increased danger of LEO interference with the GSO satellite. In addition, there may be interference between LEO satellites and ground mobile communications, as well as interference amongst LEO constellation systems. The interference process is also particularly complicated since LEO satellites are in a movable condition.

B. Motivations of Applying SG in LEO Satellite Networks

Stochastic geometry(SG) is a rich branch of applied probability theory, particularly suited to the research of random phenomena in the plane or in higher dimensions. SG has been widely used as a powerful mathematical tool in modeling and analysis of communication networks, because it is suitable for wireless networks' inherent spatial randomness and uncertainty of signals [6]. Meanwhile, it is easier for researchers to use and understand for its closed-form expressions. And most importantly, it has been proved that the lower bound of coverage probability and average achievable rate in the SG model is as tight as the upper bound of the regular mesh model [7], which means SG has much higher efficiency. The advantages of SG-based modeling and analysis in LEO satellite systems are as follows.

First, it is clear from the above survey that the number of LEO satellites will explode in the future. For such a large system, fine-grained modeling of each LEO satellite requires a lot of effort. Performing a system-level analysis based on SG is much easier than defining and studying the behavior of each satellite. SG modeling does not need to rely on orbit metrics and the shape of a particular constellation. The explosive growth of dynamic networks requires a generalized and flexible stochastic network [8].

In addition, it is clear from the above analysis of the future challenges of the LEO satellite system that the research of the impact of interference on the system performance will be an important aspect, but other than SG there is still a lack of practical analysis tools to model the interference caused by satellites.

Besides, SG is applicable to modeling and analysis of irregular topological networks [9]. In the existing non-SG models, satellites are often deployed in regular circular or hexagonal cells with the same coverage [10]. However, the distribution of satellites depends on latitude, and the coverage of satellites varies greatly in most cases. Therefore, the results of traditional analysis methods may differ significantly from the actual situation.

And eventually, for the LEO satellite system, the performance of the SG model closely matches with that of the deterministic constellation in coverage probability and average achievable rate [11].

II. SG-BASED ANALYTICAL FRAMEWORK

A. Models of Satellite Locations Distribution

In most of the available literature, satellites as well as users, satellite gateways(GWs) are assumed to be independent and uniformly distributed.

For Poisson point process (PPP), the number of points in a predefined region is Poisson distributed, while their locations are uniformly distributed within the region. As one of the most commonly used point processes, PPP can fit the ground network well in performance analysis [12]. And the coverage radius of GWs is negligible compared to the surface area of the earth, so GWs can be considered as points located in a large two-dimensional plane, PPP is suitable for modeling their locations [13].

Although PPP is highly practical, it is not the best choice for modeling finite area networks with a finite number of nodes because the satellite positions are on a sphere and the number of satellites is fixed for deterministic constellations. Therefore, modeling satellite positions as a binomial point process (BPP) is an effective solution [11], [14]. Specifically, it places a fixed number of points on a sphere of fixed height. The zenith (elevation) and azimuth angles are uniformly distributed.

In summary, the current main distribution model is that LEO satellites form independent BPP, distributed on different spheres, while terrestrial GWs form PPP.

B. Channel Model

The linear expression of the received power is $\rho\eta Cr^{-\alpha}$, where ρ is used to describe the transmitted power and antenna gain, η is used to describe large-scale fading, C is used to describe small-scale fading, and α is called the path loss exponent.

In the downlink transmission, the signal power transmission always uses this model: satellites have a larger gain in a particular direction realized by beamforming (BF) technology [15]. The GW or user can receive main-lobe power in this model, while the power from the interfering source tends to be side-lobe, which can improve the signal-to-interference ratio (SIR) of the system [16].

The path loss exponent is a number between 2 and 4 usually.

Large-scale fading is usually modeled as a log-normal shadowing to describe additional gain. Some of the literature takes the attenuation of air absorption caused by the resonance of water vapor into consideration [13][16], which is called rain attenuation. It changes with geographical location, such as desert and rain forest.

Small-scale fading is a random variable that denotes the channel fading power gains. In ideal free space propagation, small-scale fading does not occur. Shadowed-Rician (SR) fading is the most accurate channel fading model and is widely applied to make accurate performance estimates [17][18], especially for space-to-ground links [13].

When LEO satellites rely on a ground GW as a relay, a user is covered by a satellite when both satellite-GW and GW-user links achieve the SINR requirements [13].

C. Contact Distance

The distance between the user or GW and the connected (service-providing) satellite is known as the contact distance. Two expressions of the contact distance distribution for BPP are given in reference [11]. The contact distance is the distance between the user and the closest satellite at a specific height, calculated using the strongest average received power association approach. As a random variable, the complementary cumulative distribution function (CCDF) of contact distance at do is equal to the probability that there are no satellites in the spherical cap at the intersection of spherical surface over which satellites are distributed and the cone with side length do centered at the location of the user/GW region closer to the user.

D. Coverage Probability

In this section, we study the application of SG in system performance analysis. Two related definitions for measuring system performance are:

- The signal-to-interference-plus-noise ratio (SINR) is used to measure the communication quality of the system.

- Coverage probability is defined as the probability that the SINR is larger than a predetermined acceptable threshold. It represents the probability that the system can provide reliable connections.

Once the contact distance has calculated the distance to the connected satellite, the interference is the total power of all other satellites above the horizon. The coverage probability can then be computed after obtaining the SINR. Different application contexts use different expressions to describe coverage probabilities. A user is covered by a satellite when both the satellite-GW and GW-user links meet the SINR requirements when LEO satellites use a ground GW as a relay [13].

III. ORIGINAL WORK

A. System Model

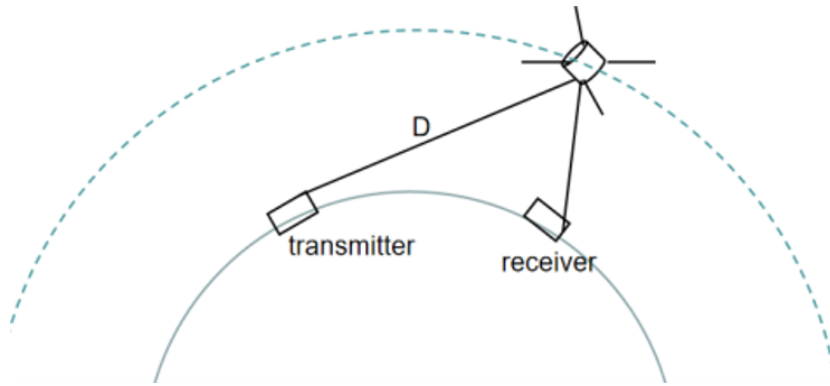


Fig. 1: T-S-R Model

In the past, many research models studied the communication from satellite to gateway and then to user, namely downlink communication. As for our group, we firstly use spherical stochastic geometry in satellite-relayed communication model, which had never been used before. That is, instead of assuming the gateway as a transmission point of information [13], a model such as transmitter-satellite-receiver(T-S-R) (Figure.1) can be analyzed independently and individually. Based on SG, we assume that the relayed satellite satisfies the BPP distribution on the low earth orbit, and the transmitter as well as the receiver on the ground satisfy the PPP distribution. This forms the SG-based analytical framework of our group. And our derivation mainly focus on finding the distance between the best relay satellite and the transmitter(D) [19]. The specific derivation steps maily refer to the steps in [13].

For our model is a simplest T-S-R relay communication model based on SG in coverage probability calculation. Such set is independent from each other, that is, we can easily extend this set of methods to multi-satellite communication chain, which is shown in the following simulation section(T-S-S-R model), and even multi-GW multi-S link communication quality analysis in the future.

B. The Obtained Formula

All assumptions as well as derivations are made in order to eventually be able to calculate the coverage probability:

$$P_{\text{cov}} = P_{\text{cov}}^{T-Sat} P_{\text{cov}}^{Sat-Re}, \quad (1)$$

where

$$P_{\text{cov}}^{T-Sat} = P \left(\frac{\rho_r^t}{\sigma_s^2} \geq \gamma_s \right), \quad (2)$$

$$P_{\text{cov}}^{Sat-Re} = P \left(\frac{\rho_r^s}{\sigma_r^2} \geq \gamma_r \right), \quad (3)$$

σ_s^2 and σ_r^2 are the noise powers at the satellite and the receiver, respectively [13].

To simplify the model, we assume that the communication from the transmitter to the satellite is influenced by the same factors as the communication from the satellite to the receiver, and the other parameters should be the same excluding the influence of such a factor as distance. Therefore, first of all, we try to deduce the contact distance. Here we only discuss the distance from the transmitter to the satellite (D), for the distance from the satellite to the receiver can be deduced in the same way. The globe uses a spherical coordinate system, so we first use angles to express geometric relations, and then use the law of cosines to convert angles into distances.

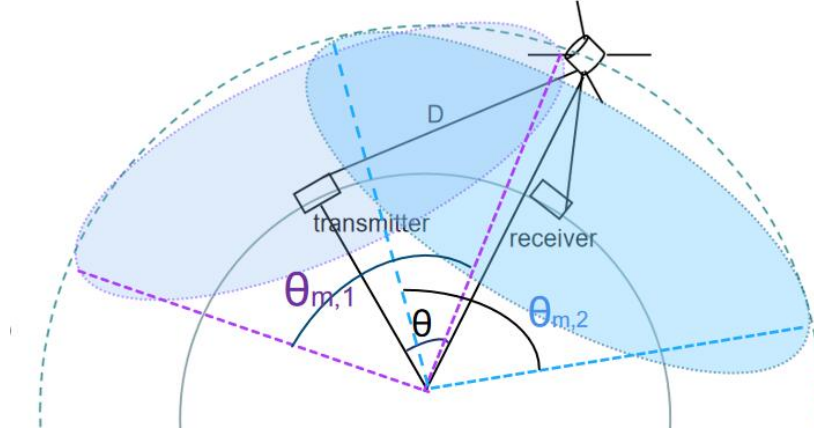


Fig. 2: Satellite-relayed communication model (T-S-R)

As shown in Figure.2, we suppose θ is the angle between the transmitter and the satellite and the center of the earth. The derivation is as follows:

- Fix the receiver's position, its dome angle $\theta_{m,2}$ and coverage area A_2
- Change the position of the transmitter, its dome angle $\theta_{m,1}$ and coverage area A_1 will change too [20]. Under such changes, there is an overlap between A_1 and A_2 .
- According to the distribution of satellites, judge whether the transmitter can find a satellite that can successfully communicate in the overlapping area and calculate the probability of no satellite.
- The coverage probability is the probability that $N-1$ satellites are not in the overlap area. Or we can call it cumulative distribution function (CDF) of contact angle. Then by using the law of cosines we replace theta with D and take the derivative of D , we can get the probability density function(PDF) of contact distance distribution.

$$\begin{aligned}
f &= \frac{1}{\sigma_2} N \left(1 - \frac{\int_{\sigma_5}^{\sigma_1} \sigma_6 dl + \int_{\sigma_8}^{R \sin(\sigma_{17})} \sigma_6 dl}{\sigma_2} \right)^{N-1} \\
&\times \left(\int_{\sigma_5}^{\sigma_1} \sigma_4 dl + \int_{\sigma_8}^{R \sin(\sigma_{17})} \sigma_4 dl + 2R \operatorname{asin} \left(\frac{\sqrt{\sigma_{13} - R^2 \sigma_{11}^2 \cos(\sigma_{17})^2}}{R} \right) \right) \\
&\times \left(\frac{D \sigma_{11} \sin(\sigma_{17})}{R_e} + R \cos(\sigma_{17}) \left(\frac{\frac{\sigma_3}{2\sigma_{15}} - \frac{2D\sigma_{16} \sin(\sigma_{17})}{RR_e}}{\cos(\sigma_{17})} + \frac{D \sin(\sigma_{17}) \sigma_{14}}{\sigma_7} \right) (\sigma_{11}^2 + 1) \right) \quad (4) \\
&- 2R^2 \cos \left(\frac{\theta_{m,2}}{2} \right) \operatorname{asin} \left(\frac{\sqrt{\sigma_{13} - R^2 \sigma_9^2 \sigma_{18}}}{R} \right) (\sigma_9^2 + 1) \\
&\times \left(\frac{\sigma_3}{2 \cos(\sigma_{17}) \sigma_{15}} + \frac{D \sin(\sigma_{17}) \sigma_{12}}{\sigma_7} \right) - \frac{2DR \operatorname{asin}(0) \cos(\sigma_{17})}{R_e}
\end{aligned}$$

where $\sigma_1 - \sigma_{18}$ are shown in Appendix A.

In addition to distance, there are other attenuation factors, such as rain attenuation, which we won't discuss too much in this section. We end up with the expression:

$$\begin{aligned}
P_{\text{cov}}^{\text{S-Sat}} &= \int_0^\infty \frac{1}{2\sqrt[4]{D}} f_{D1}(\sqrt[4]{D}) \\
&- \left(\frac{2b_0 m}{2b_0 m + \Omega} \right)^m \sum_{z=0}^\infty \frac{(m)_z}{z! \Gamma(z+1)} \left(\frac{\Omega}{2b_0 m + \Omega} \right)^z \quad (5) \\
&\times \int_0^\infty \gamma \left(z+1, \frac{1}{2b_0} c \sqrt{D} \right) \frac{1}{2\sqrt[4]{D}} f_{D1}(\sqrt[4]{D}) dD
\end{aligned}$$

$$\begin{aligned}
P_{\text{cov}}^{\text{Sat-Re}} &= \int_0^\infty \frac{1}{2\sqrt[4]{D}} f_{D1}(\sqrt[4]{D}) \\
&- \left(\frac{2b_0 m}{2b_0 m + \Omega} \right)^m \sum_{z=0}^\infty \frac{(m)_z}{z! \Gamma(z+1)} \left(\frac{\Omega}{2b_0 m + \Omega} \right)^z \quad (6) \\
&\times \int_0^\infty \gamma \left(z+1, \frac{1}{2b_0} c \sqrt{D} \right) \frac{1}{2\sqrt[4]{D}} f_{D1}(\sqrt[4]{D}) dD
\end{aligned}$$

where $\Gamma(\cdot)$ denotes the gamma function, $\gamma(\cdot, \cdot)$ is the lower incomplete gamma function, $(m)_z$ is the Pochhammer symbol, while m , b_0 and Ω are the parameters of the SR fading [13].

IV. SG-BASED SIMULATION SETUP AND NUMERICAL RESULTS

A. Simulation Model

We simulate this stochastic geometry process with the Monte Carlo method to evaluate the coverage probability of satellite-relayed system.

TABLE II: System Parameters

PRAMETER	VALUE
Surface background noise	-80dB
Background noise in space 550km from the earth's surface	-100dB
Average rain attenuation	-2dB
Lobe angel of the ground-based antenna	$\frac{65}{180}\pi$
Ground gateway antenna gain	80dB
Satellite antenna gain	60dB
SR fading(Ω, b_0, m)	SR(1.29, 0.158, 19.4)
Carrier frequency	300MHz

Assume that there are gateways conforming to a PPP with a surface density of λ_{GW} distributed over the Earth's surface. Assume that a fixed quantity of LEO satellites conforming to a BPP distribution are distributed in a fixed LEO. Consider a gateway-satellite-gateway(T-S-R) downlink relay communication system with the same receiving antenna and transmitting antenna of the gateway. And consider that there is an overlap between the region swept by the width of the wave flaps of the receiving and transmitting station antennas to establish a link. Rain fading, propagation fading, and antenna gain for signal strength occur in both T-S and S-R links. In the S-S link only propagation attenuation and antenna gain occur. And it is assumed that the antenna gain, the Earth's surface, and the background noise of the space in which the LEO satellite is located are a constant.

B. Simulation Details

- 1) *Selection of relay satellite*: To ensure the successful transmission of the transmit signal to the relay satellite as much as possible, the relay satellite is selected to be the closest satellite to the transmitting station in the effective overlap region of the wave flaps between the transmitting and receiving stations.
- 2) *SR fading*: the following lemma from [13]:

$$F_D(d) = P(D < d) = 1 - \prod_{i=1}^n P(D_i \geq d), \quad (7)$$

Since it contains the summation using the 50th order incomplete gamma function, the inverse function cannot be taken directly. So it is first fitted with a 10th order polynomial in the function value (0-1) increasing curve (rounding off both ends), after which the

inverse is taken, after which the SR distribution can be generated using uniform random numbers

- 3) *Simulation of spherical BPP and PPP*: The total number of random points of PPP is obtained from the Poisson distribution in one dimension, after which the random points still conform to BPP, and the following equation is obtained by taking the inverse function of the CDF of the sphere coordinates of the uniformly distributed points using the sphere. Then use the uniform random number to generate the point process.
- 4) *Calculation of coverage probability*: The probability that the ratio of transmitter's transmit power to receiver's receive power is greater than the threshold γ is the coverage probability. In this paper, the coverage probabilities of T-S-R process and S-R process with valid link occurrence, and the coverage probabilities of T-S-R process and T-S-S-R process with arbitrary gateway communication without ensuring valid link occurrence are considered respectively.
- 5) *The practical optimization of the introduction of satellite-satellite links for the premise of not ensuring the effective occurrence of the link*:

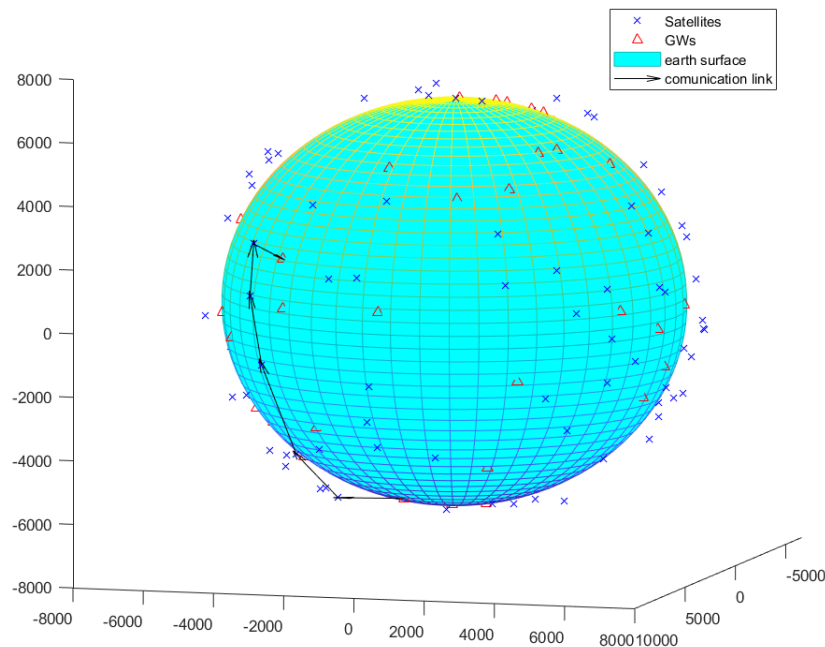


Fig. 3: Satellite communication(T-S-S-R model)

The introduction of a satellite-satellite communication link makes it possible for any two

gateways on the earth's surface to establish a communication link. The signal is sent from the transmitting station to the nearest satellite, through the satellite-satellite link, and finally to the receiving station when it reaches within the antenna flap width of the target receiving station. Although there is some fading and delay, this greatly increases the coverage probability of establishing communication between any gateways. Where the satellite link selection is obtained by a local greedy algorithm. The spherical coordinate system is transformed into the two-dimensional matrix shown in the figure. Set the local distance threshold d_{max} , the current starting point to the end point vector $\nu - target$, and find the satellite point location within the range that makes the smallest angle with $\nu - target$ as the new starting point each time, and iterate to get the satellite link.

C. Comparison and Analysis of Numerical Results

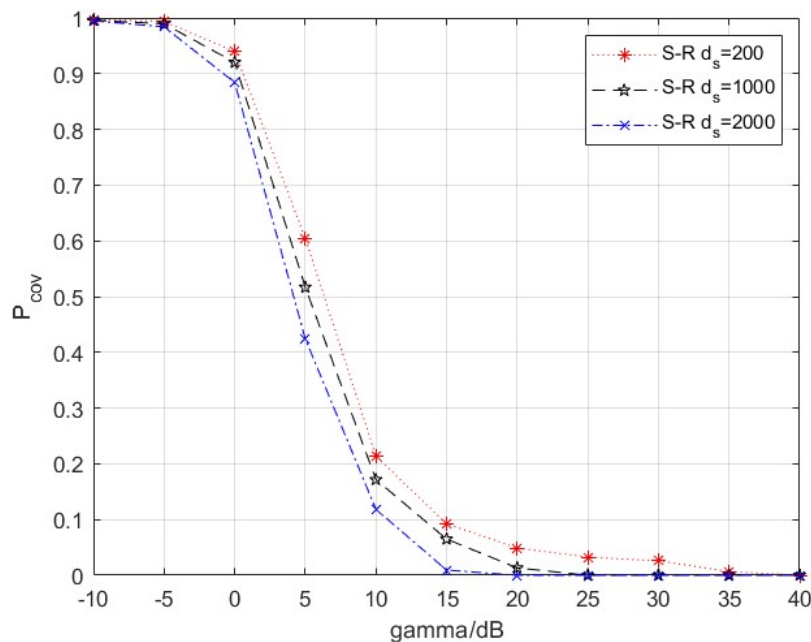


Fig. 4: $\lambda_{GW} = 1.96e^{-7}/km^{-2}$; $\theta_m = \frac{65}{180}\pi$; $N_S = 100000$

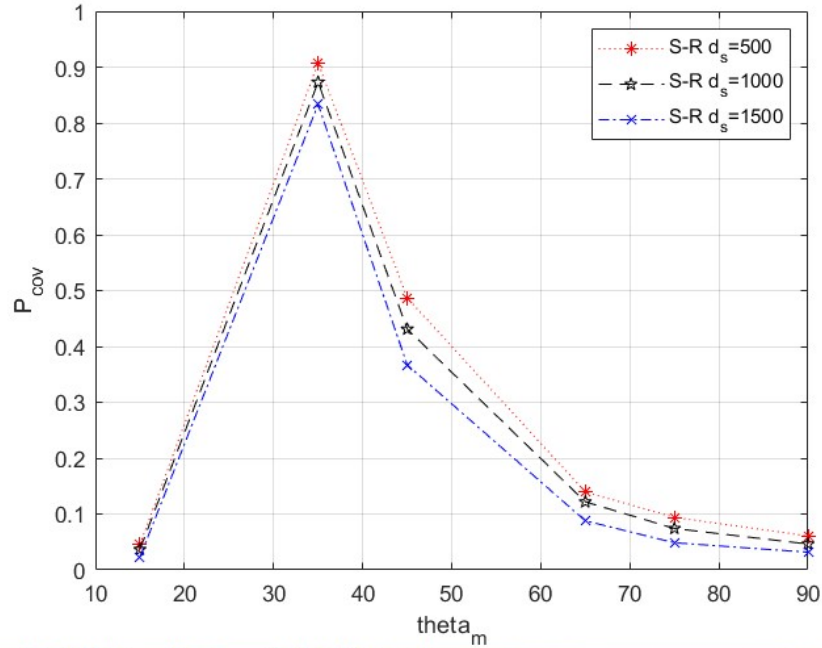


Fig. 5: $\gamma = 12dB$; $\lambda_{GW} = 1.96e^{-7}/km^{-2}$

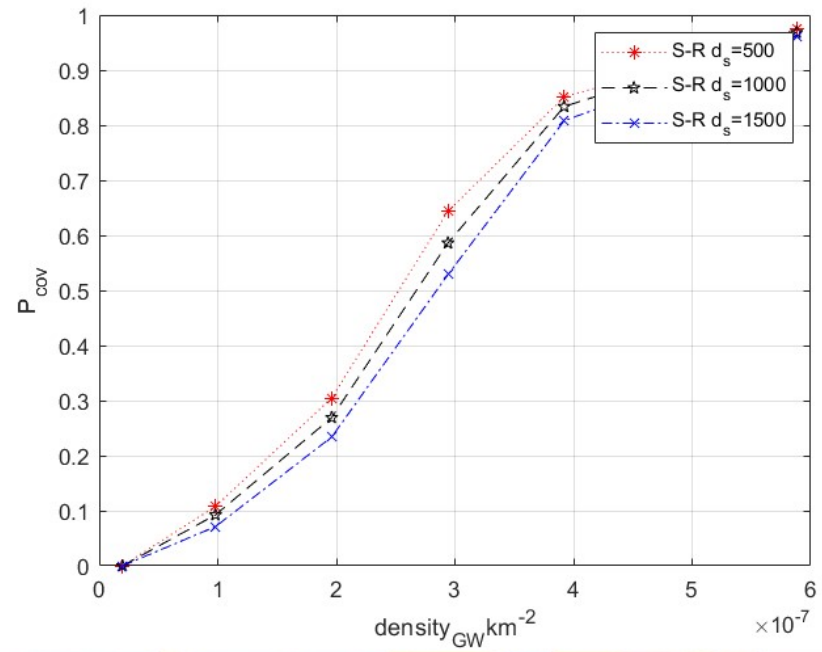


Fig. 6: $\gamma = 12dB$; $N_s = 100000$

From the Figure 4 5 6 it can be seen that the effect of changing d_s alone on the S-R coverage probability of a single relay communication is not significant when N_s is fixed to a certain value.

From the subsequent analysis we can learn that d_s is strongly correlated with N_s .

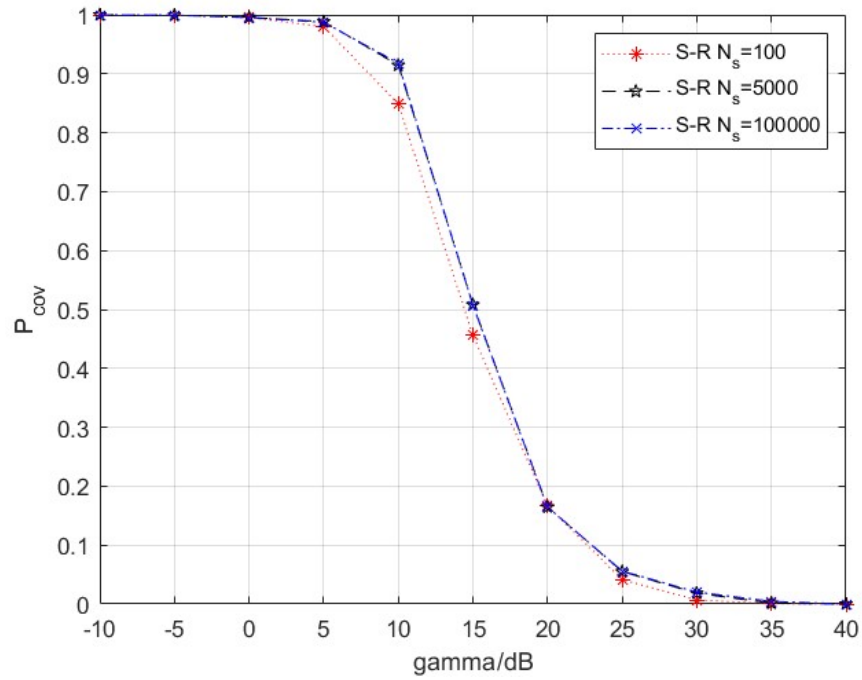


Fig. 7: $d_s = 550km$; $\lambda_{GW} = 1.96e^{-7}/km^{-2}$

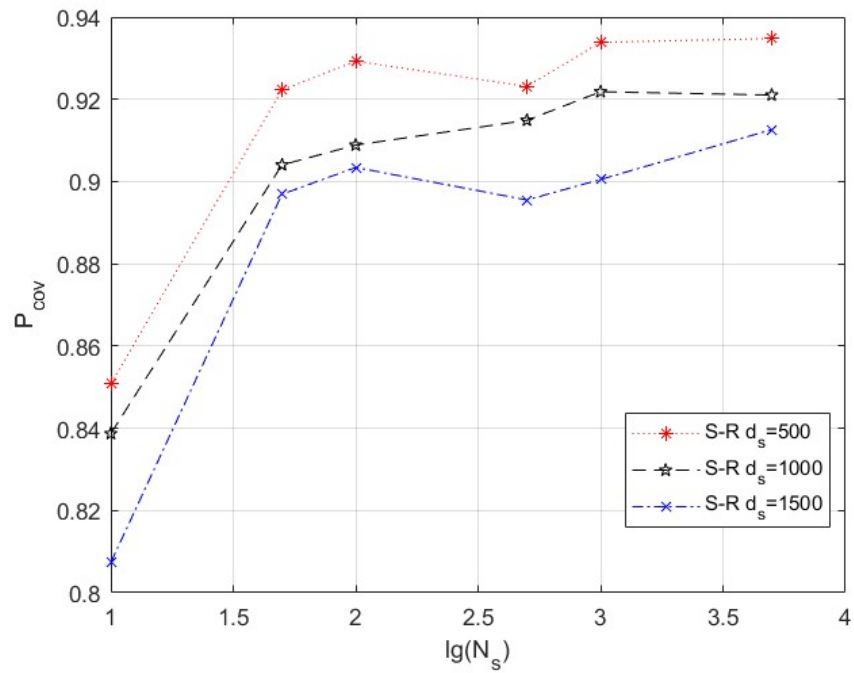


Fig. 8: $\gamma = 12dB$; $\lambda_{GW} = 1.96e^{-7}/km^{-2}$

Figure 7 illustrates that with $d_s=550\text{km}$; $\text{density}_{GW}=\frac{100}{4\pi R_e^2}$, the number of satellites is saturated for a single communication to be able to achieve complete coverage. However, it should be noted that the saturation of coverage probability only indicates that the communication quality must be guaranteed, but it does not guarantee the time delay. Because once the regional satellites are fully occupied, the waiting time will be huge.

Figure 8 shows that the number of satellites in fixed orbits, the lower the orbital altitude the higher the coverage probability. The coverage probability increases with a fixed orbital altitude and a higher number of orbiting satellites, but saturates after reaching a certain value, the same result as shown in Figure 4 5 6. It is also clearly shown that as the orbital altitude increases, the number of satellites required to reach the same coverage probability increases rapidly.

Fig. 9: T-S-R coverage probability between arbitrary gateways

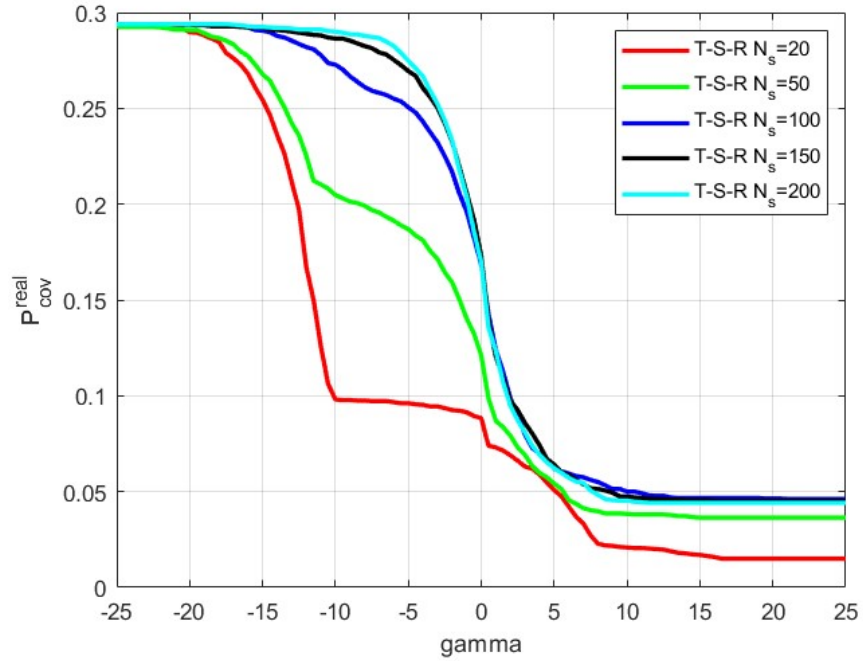


Fig. 10: T-S-S-R coverage probability between arbitrary gateways

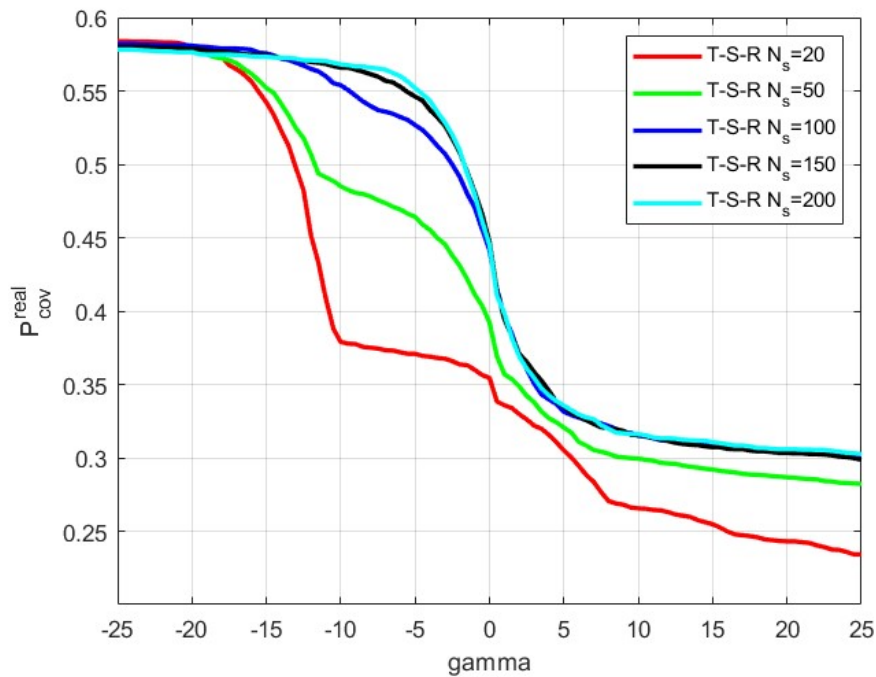


Fig. 11: Coverage probability between arbitrary GWs(T-S-R+T-S-S-R)

The previously obtained results are coverage probabilities calculated from the SNR of the communication process under the premise of ensuring the overlap between the receiving station

and the transmitting station's flap width sweep area, while here the coverage probability between any two gateways is analyzed. It can be clearly seen that the contribution of the communication link between the satellites to the coverage probability is significant, and this contribution increases with the number of satellites and saturates after reaching a certain value.

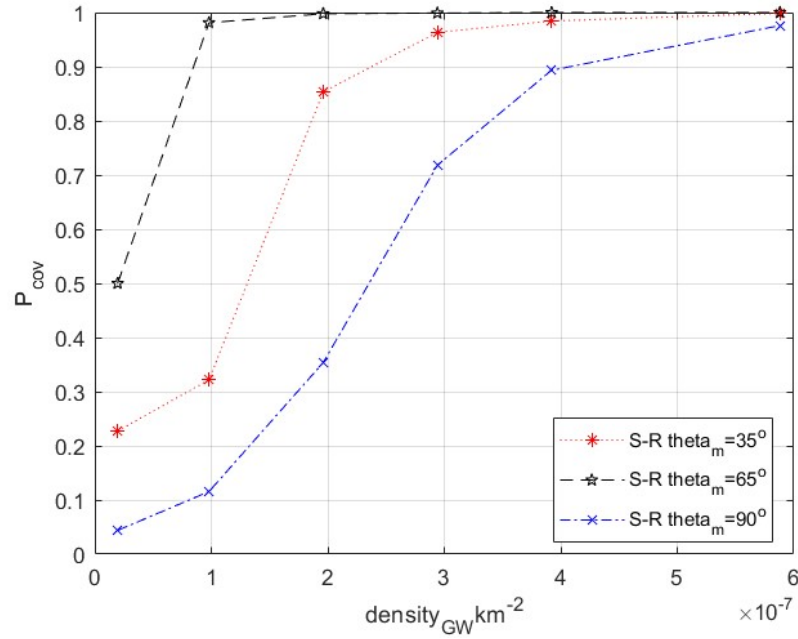


Fig. 12: $\gamma = 12dB$; $ds = 550km$

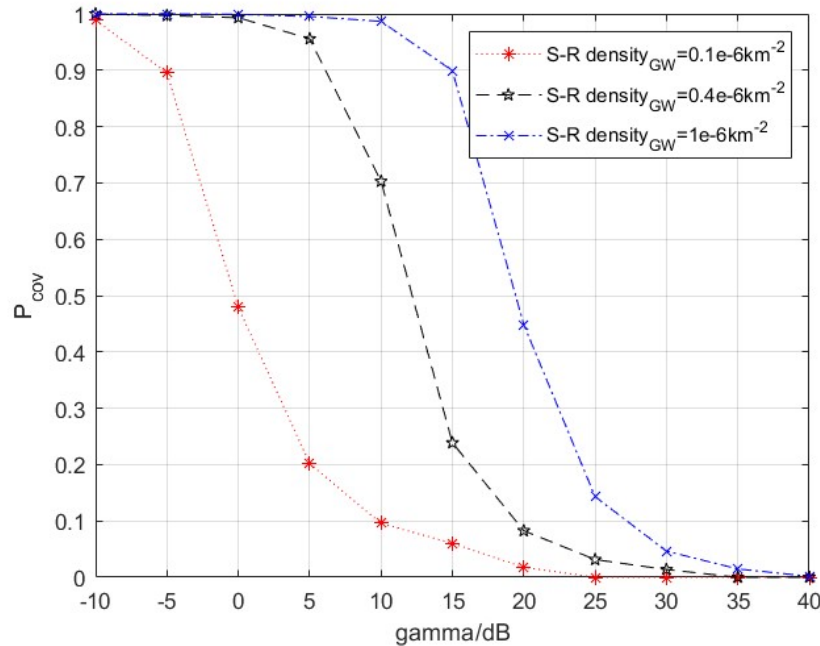


Fig. 13: $\theta_m = \frac{65}{180}\pi$; $N_s = 100000$; $d_s = 550km$

Figure 12 shows that the width of the lobe required to achieve the same coverage probability increases as the ground gateway density increases. and that the coverage probability increases significantly as the lobe decreases, and that the coverage probability increases significantly as the gateway density increases.

Figure 13 shows more clearly in case of $\theta_m = \frac{65}{180}\pi$; $N_s = 100000$; $d_s = 550km$, the relationship between coverage probability, threshold and density.

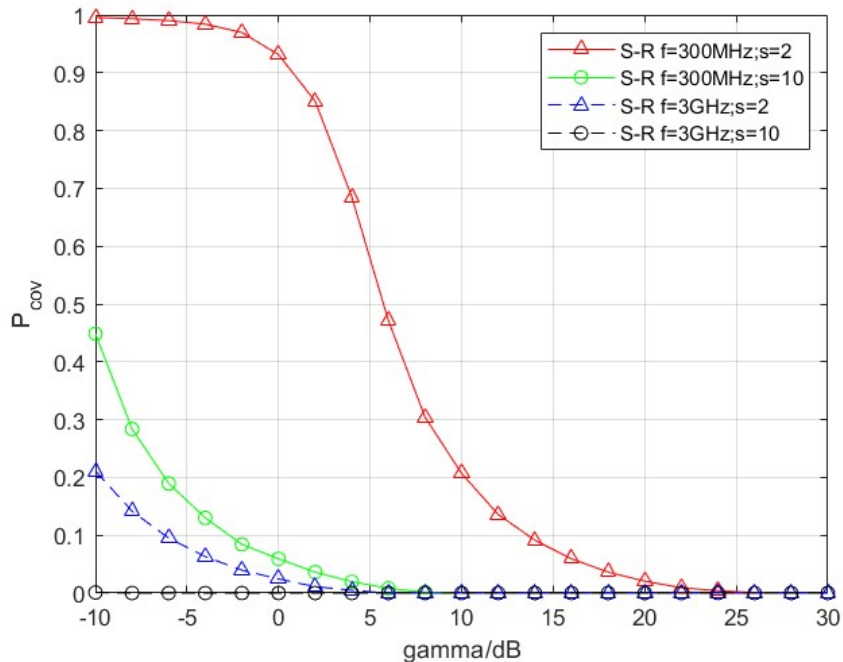


Fig. 14: $N_{GW} = 100$; $N_s = 100$

Figure 14 shows the effect of carrier frequency and rain attenuation on the coverage probability. The rain attenuation coefficient at this point depends only on the depolarization process of raindrops for the carrier, because the scattering effect of raindrops can be neglected due to the long wavelength of the UHF band we have chosen. We can obviously under the existing model assumptions, the increase of frequency and the enhancement of rain attenuation effect is significant for the coverage probability. However, in the actual process, the effect brought by the change of frequency can be improved due to the enhancement of the gain circuit for the amplification effect of high frequency.

V. CONCLUSIONS AND FUTURE APPLICATIONS

This article investigates the application of SG to simulating and analyzing LEO satellite communications systems, introduces several satellite distributions, and analyzes the channel models in the literature. From a non-technical perspective, we describe contact distance and coverage probability. Then, we use the satellite-relayed communication model based on SG to derive the PDF of the contact distance between the transmitter and the satellite(T-S link) and the probability of successful communication (coverage probability) in T-S-R model. A series of simulations are made on this model and the following conclusions are obtained. Increasing the

TABLE III: Table of Notations and Acronyms

Notations	Description
LEO, GEO	Low, Geostationary Earth Orbit
SG	Stochastic Geometry
GW	Gateway
BPP, PPP	Binomial Point Process, Poisson Point Process
SINR	Signal-to-interference-plus-noise ratio
SIR	Signal-to-interference ratio
SR fading	Shadowed-Rician fading
$P_{cov}^{T-Sat}, P_{cov}^{Sat-Re}$	Coverage probability for T-S link, S-R link
ρ_r^t, ρ_r^s	Transmitter power, Satellite power
σ_s^2, σ_r^2	Noise power at the satellite, at the receiver
γ_s, γ_r	SNR threshold at the satellite, at the receiver
D	Length of T-S link
R, Re	The radius of the sphere, the Earth
θ_m	The Dome angle
A_1, A_2	Shaded area of transmitter, receiver
θ	The angle between the transmitter and the satellite and the center of the earth
CDF	Cumulative distribution function
PDF	Probability density function
λ_{GW}	The surface density of GW in PPP
ds	Altitude of LEO
N_S	Number of satellites in fixed orbit
γ	Equals to γ_s or γ_r
f	Carrier frequency
s	Average rain attenuation

number of satellites and the height of the constellation within a specific range can effectively promote the coverage probability. The ability of the satellites to communicate with each other has a considerable effect on promoting the coverage probability. This indicates that the recent technological advances in enabling S-S communications will significantly widen the set of applications that can rely on LEO satellite communications.

High altitude platforms (HAPs) are airborne base stations placed in the stratosphere by airships or drones, combining the advantages of satellite communication systems and ground mobile cellular networks. Due to the greater distance from the ground, the number of satellites required to complete the communication coverage is less, and the coverage radius is larger than that of the ground mobile system, which can save costs and also accomplish a certain quality of high-capacity communication [21]. However, its disadvantages are also obvious: stronger rain fading attenuation, the need to use higher frequency bands; the multipath effect will affect the user's received power, and the path loss is large [22]. There is no relevant paper studying HAPs by using SG, but there is a high possibility of future research in this area.

APPENDIX A

THE EXPRESSIONS OF σ

$$\sigma_1 = R \sin \frac{\theta_{m,2}}{2} \quad (8)$$

$$\sigma_2 = 4\pi R^2 \quad (9)$$

$$\sigma_3 = \sqrt{2} \left(\frac{2D \cos(\sigma_{17}) \sin(\sigma_{17})}{RR_e} - \frac{2D \cos\left(\frac{\theta_{m,2}}{2}\right) \sin(\sigma_{17})}{RR_e} + \frac{2D \cos\left(\frac{\theta_{m,2}}{2}\right) \sigma_{16}^2 \sin(\sigma_{17})}{RR_e} \right) \quad (10)$$

$$\sigma_4 = -\frac{2DR \cos(\sigma_{17}) \sin(\sigma_{17})}{R_e \sqrt{1 - \frac{\sigma_{13} - l^2}{R^2} \sigma_{10}}} \quad (11)$$

$$\sigma_5 = -R\sigma_9 \cos\left(\frac{\theta_{m,2}}{2}\right) \quad (12)$$

$$\sigma_6 = 2R \operatorname{asin}\left(\frac{\sigma_{10}}{R}\right) \quad (13)$$

$$\sigma_7 = RR_e \cos(\sigma_{17})^2 \quad (14)$$

$$\sigma_8 = -R\sigma_{11} \cos(\sigma_{17}) \quad (15)$$

$$\sigma_9 = \tan\left(\cos\left(\frac{\theta_{m,2}}{2}\right) + \frac{\sigma_{12}}{\cos(\sigma_{17})}\right) \quad (16)$$

$$\sigma_{10} = \sqrt{\sigma_{13} - l^2} \quad (17)$$

$$\sigma_{11} = \tan\left(\cos\left(\frac{\theta_{m,2}}{2}\right) - \frac{\sigma_{14}}{\cos(\sigma_{17})}\right) \quad (18)$$

$$\sigma_{12} = 2 \cos\left(\frac{\theta_{m,2}}{2}\right) \sigma_{16} - \sqrt{2} \sigma_{15} \quad (19)$$

$$\sigma_{13} = R^2 \sin(\sigma_{17})^2 \quad (20)$$

$$\sigma_{14} = 2\sigma_{16} \cos(\sigma_{17}) - \sqrt{2} \sigma_{15} \quad (21)$$

$$\sigma_{15} = \sqrt{\sigma_{18} + 2 \cos\left(\frac{\theta_{m,2}}{2}\right) \sigma_{16}^2 \cos(\sigma_{17}) - 2 \cos\left(\frac{\theta_{m,2}}{2}\right) \cos(\sigma_{17}) + \cos(\sigma_{17})^2} \quad (22)$$

$$\sigma_{16} = \text{asin}\left(\frac{d}{2R_e}\right) \quad (23)$$

$$\sigma_{17} = \frac{-D^2 + R^2 + R_e^2}{2RR_e} \quad (24)$$

$$\sigma_{18} = \cos\left(\frac{\theta_{m,2}}{2}\right)^2 \quad (25)$$

REFERENCES

- [1] S. Cakaj, B. Kamo, A. Lala, and A. Rakipi, "The coverage analysis for low earth orbiting satellites at low elevation," *International Journal of Advanced Computer Science and Applications*, vol. 5, no. 6, 2014. [Online]. Available: <http://dx.doi.org/10.14569/IJACSA.2014.050602>
- [2] P. K. Sharma, P. K. Upadhyay, D. B. da Costa, P. S. Bithas, and A. G. Kanatas, "Performance analysis of overlay spectrum sharing in hybrid satellite-terrestrial systems with secondary network selection," *IEEE Transactions on Wireless Communications*, vol. 16, no. 10, pp. 6586–6601, 2017.
- [3] B. E. Y. Belmekki and M.-S. Alouini, "Unleashing the potential of networked tethered flying platforms: Prospects, challenges, and applications," *IEEE Open Journal of Vehicular Technology*, vol. 3, pp. 278–320, 2022.
- [4] S. Michael and P. Magdalena, "Why in the next decade companies will launch thousands more satellites than in all of history," *Wm. & Mary L. Rev.*, vol. 62, p. 324, 2019.
- [5] P. Chini, G. Giambene, and S. Kota, "A survey on mobile satellite systems," *International Journal of Satellite Communications and Networking*, vol. 28, no. 1, pp. 29–57, 2010.
- [6] H. ElSawy, A. Sultan-Salem, M.-S. Alouini, and M. Z. Win, "Modeling and analysis of cellular networks using stochastic geometry: A tutorial," *IEEE Communications Surveys & Tutorials*, vol. 19, no. 1, pp. 167–203, 2017.
- [7] J. G. Andrews, F. Baccelli, and R. K. Ganti, "A tractable approach to coverage and rate in cellular networks," *IEEE Transactions on Communications*, vol. 59, no. 11, pp. 3122–3134, 2011.
- [8] R. Wang, M. A. Kishk, and M.-S. Alouini, "Ultra-dense LEO satellite-based communication systems: A novel modeling technique," *IEEE Communications Magazine*, vol. 60, no. 4, pp. 25–31, 2022.
- [9] M. Haenggi, *Stochastic Geometry for Wireless Networks*. Cambridge University Press, 2012.
- [10] H. Mourad, A. Al-Bassiouni, S. Emam, and E. Al-Hussaini, "Generalized performance evaluation of low earth orbit satellite systems," *IEEE Communications Letters*, vol. 5, no. 10, pp. 405–407, 2001.
- [11] N. Okati, T. Riihonen, D. Korpi, I. Angervuori, and R. Wichman, "Downlink coverage and rate analysis of low earth orbit satellite constellations using stochastic geometry," *IEEE Transactions on Communications*, vol. 68, no. 8, pp. 5120–5134, 2020.
- [12] Z. Lou, A. Elzanaty, and M.-S. Alouini, "Green tethered UAVs for EMF-aware cellular networks," *IEEE Transactions on Green Communications and Networking*, vol. 5, no. 4, pp. 1697–1711, 2021.
- [13] A. Talgat, M. A. Kishk, and M.-S. Alouini, "Stochastic geometry-based analysis of leo satellite communication systems," *IEEE Communications Letters*, vol. 25, no. 8, pp. 2458–2462, 2021.
- [14] R. Wang, M. A. Kishk, and M.-S. Alouini, "Evaluating the accuracy of stochastic geometry based models for LEO satellite networks analysis," *arXiv preprint arXiv:2207.12029*, 2022.

- [15] X. Zhang, Z. Zheng, W.-Q. Wang, and H. C. So, "DOA estimation of mixed circular and noncircular sources using nonuniform linear array," *IEEE Transactions on Aerospace and Electronic Systems*, 2022.
- [16] B. A. Homssi and A. Al-Hourani, "Modeling uplink coverage performance in hybrid satellite-terrestrial networks," *IEEE Communications Letters*, vol. 25, no. 10, pp. 3239–3243, 2021.
- [17] A. Abdi, W. Lau, M.-S. Alouini, and M. Kaveh, "A new simple model for land mobile satellite channels: first- and second-order statistics," *IEEE Transactions on Wireless Communications*, vol. 2, no. 3, pp. 519–528, 2003.
- [18] G. Alfano and A. De Maio, "Sum of squared shadowed-rice random variables and its application to communication systems performance prediction," *IEEE Transactions on Wireless Communications*, vol. 6, no. 10, pp. 3540–3545, 2007.
- [19] K. Belbase, Z. Zhang, H. Jiang, and C. Tellambura, "Coverage analysis of millimeter wave decode-and-forward networks with best relay selection," *IEEE Access*, vol. 6, pp. 22 670–22 683, 2018.
- [20] R. Wang, M. A. Kishk, and M.-S. Alouini, "Stochastic geometry-based low latency routing in massive leo satellite networks," *arXiv preprint arXiv:2204.03802*, 2022.
- [21] A. Mohammed, A. Mehmood, F.-N. Pavlidou, and M. Mohorcic, "The role of high-altitude platforms (haps) in the global wireless connectivity," *Proceedings of the IEEE*, vol. 99, no. 11, pp. 1939–1953, 2011.
- [22] X. Zhang, Z. Zheng, W.-Q. Wang, and H. C. So, "DOA estimation of coherent sources using coprime array via atomic norm minimization," *IEEE Signal Processing Letters*, 2022.